

Neutron electric dipole moment with two flavors of domain wall fermions*

F. Berruto

Brookhaven National Laboratory

Tom Blum[†]

University of Connecticut

E-mail: tblum@phys.uconn.edu

K. Orginos

Massachusetts Institute of Technology

A. Soni

Brookhaven National Laboratory

We present a study of the neutron electric dipole moment (\vec{d}_N) within the framework of lattice QCD with two flavors of light quarks. The dipole moment is sensitive to the topological structure of the gauge fields, so accuracy can only be achieved by using dynamical, or sea quark, calculations. The topological charge (distribution) evolves slowly in these calculations, leading to systematic uncertainty in \vec{d}_N . It is shown, using quenched configurations, that a better sampling of the charge distribution eliminates this problem, but because the CP even part of the fermion determinant is absent, both the topological charge distribution and \vec{d}_N are pathological in the chiral limit. We discuss the systematic uncertainties arising from the topological charge distribution and unphysical quark mass in our calculations and prospects for eliminating them.

Our calculations are done using two flavors of domain wall fermions and the DBW2 gauge action with inverse lattice spacing $a^{-1} \approx 1.7$ GeV, physical volume $V \approx (2 \text{ fm})^3$, and light quark mass roughly equal to the strange quark mass. The systematic uncertainties described above notwithstanding, we find $|\vec{d}_N| = 10(11) \times 10^{-15} e \text{ cm}$. The central value translates into the bound $\theta \lesssim 6.3 \times 10^{-11}$ on the fundamental CP-odd parameter in the QCD lagrangian when combined with the current experimental bound on $|\vec{d}_N|$. The quoted error is statistical only. Satisfactory results for the magnetic dipole moments and electromagnetic form factors of the proton and neutron are also obtained.

XXIIIrd International Symposium on Lattice Field Theory

25-30 July 2005

Trinity College, Dublin, Ireland

*We thank RIKEN, Brookhaven National Laboratory, and the U.S. Department of Energy for providing the facilities and resources necessary to complete this work.

[†]Speaker.

1. Introduction

One of the most intriguing aspects of quantum chromodynamics (QCD) is that it allows a gauge invariant interaction term that is separately odd under time-reversal (T) and parity (P) transformations, the so-called θ term. The presence of such a term has the profound effect that the Strong interactions violate the combined symmetry charge-conjugation (C) times P. The existence of P and T violating interactions in the action imply permanent electric dipole moments for fundamental particles. Presently, the most precise search for a permanent electric dipole moment comes from the measurement of the electric dipole moment of the neutron, \vec{d}_N . In the Standard Model, the CP-odd phase of the CKM mixing matrix also produces a non-vanishing value for \vec{d}_N , but only beyond one loop order in the Weak interaction. Consequently, this contribution to \vec{d}_N is estimated to be less than $10^{-30} e\text{-cm}$, many orders of magnitude below the current experimental bound[1], $d_N = |\vec{d}_N| < 6.3 \times 10^{-26} e\text{-cm}$ (see also [2]). There are recent proposals to improve this bound by two to three orders of magnitude by studying the electric dipole of the deuteron at Brookhaven National Laboratory[3] and an isotope of radium (^{225}Ra) at Argonne National Laboratory [4]. The latter is now underway.

Using this experimental bound with theoretical estimates of d_N/θ [5, 6, 7, 8, 9, 10], then implies a bound on the value of the fundamental CP-odd parameter in the QCD action, $\theta \lesssim 10^{-10}$, which is deemed to be unnaturally small. Since there is no good reason for this number to be so different from unity (*i.e.*, a heretofore unknown symmetry of Nature), its minuteness requires “fine-tuning” of the action. This is often termed the Strong CP problem.

In this talk we present a calculation of d_N in units of θ in QCD with two flavors of light quarks using the lattice regularization. We note that while finishing this work, a similar study, but in the quenched approximation, has appeared in [11] and was also summarized in a talk at this meeting by E. Shintani. As explained below, the electric dipole moment is sensitive to the topology of the gauge field, or more specifically, fluctuations of topological charge; thus we focus mainly on calculations with dynamical, or sea, quarks. The two flavor ensemble of lattice gauge fields that we use was generated by the RIKEN BNL Columbia collaboration. Details of these simulations are described in [12]. We find that a precise and accurate calculation requires ensembles with significantly longer evolutions (*i.e.*, more independent configurations) than presently available; the topological charge has very long auto-correlations. We expect that longer evolutions will be available in the near future¹. This situation is to be compared to the quenched, or zero flavor, case where topological charge can be evolved more efficiently. The topological charge susceptibility, however, does not vanish as the valence quark mass approaches the chiral limit, and as we show, neither does the electric dipole moment. This quenched pathology means d_N can only be accurately calculated when the sea quarks are included[13]. Not surprisingly, this was also found to be true in a recent work using the instanton liquid model[10].

Since topology is crucial in the calculation of d_N , it may also be important to use lattice fermions that do not spoil certain topological relations to the gauge field with large lattice spacing errors. The axial anomaly in QCD relates the topological charge to the pseudoscalar density; a chiral rotation on the quark fields in the QCD action shifts the CP-odd θ term between gluon and

¹The RBC and UKQCD collaborations are jointly beginning extensive simulations with 2+1 flavors of domain wall fermions.

quark sectors. In order to realize this proper behavior, we use domain wall fermions which are chirally symmetric even when the lattice spacing is non-vanishing. Thus, this important continuum property of QCD is realized at non-zero lattice spacing, a feature that is much more difficult for Wilson- and staggered- type fermions.

2. Theoretical background

We begin by considering the addition of a T- and P-odd (therefore CP-odd) term to the QCD Lagrangian:

$$S_{QCD,\theta} = -\theta \int dt \int d^3x \frac{g^2}{32\pi^2} \text{tr} [\varepsilon_{\mu\nu\rho\sigma} G^{\rho\sigma}(\vec{x},t) G^{\mu\nu}(\vec{x},t)], \quad (2.1)$$

where $G_{\mu\nu}$ is the gluon field strength and the trace is over (suppressed) color indices. Such a term is allowed by the gauge, Lorentz, and discrete symmetries of QCD. It is easy to see this so-called θ term is odd under P and T transformations since $\varepsilon_{\mu\nu\rho\sigma} G^{\rho\sigma} G^{\mu\nu} \sim \vec{E} \cdot \vec{B}$. θ is a fundamental, but unknown parameter of QCD. Remarkably, even though Equation 2.1 can be written as a total divergence, it does not vanish[14] and therefore has physical consequences, most notably CP violation in QCD. We return to this shortly.

On the other hand, the QCD Lagrangian for massless fermions is invariant under chiral transformations of the quark fields,

$$\psi \rightarrow (1 + i\phi\gamma_5/2)\psi, \quad \bar{\psi} \rightarrow \bar{\psi}(1 + i\phi\gamma_5/2), \quad (2.2)$$

but the measure of the path intergral is not[15].

$$\mathcal{D}\psi\mathcal{D}\bar{\psi} \rightarrow \mathcal{D}\psi\mathcal{D}\bar{\psi} \exp \left\{ i\phi \int d^4x \frac{g^2}{32\pi^2} \text{tr} [\varepsilon^{\mu\nu\rho\sigma} G_{\mu\nu} G_{\rho\sigma}] \right\}, \quad (2.3)$$

which gives rise to the Adler-Bell-Jackiw anomaly. It is well known that this axial anomaly induces observable effects even when CP is not broken, the mass of the η' and the large decay rate for $\pi^0 \rightarrow \gamma\gamma$ to name just two. In this work we are interested in CP-violating effects, ones that vanish when the θ term is absent from the Lagrangian.

Choosing $\phi = -\theta$, the θ term can be rotated away, or canceled in the action. Recently, Creutz has proposed a scenario in the *one*-flavor theory where the θ term can not be removed, even in the massless limit[16, 17].

If all the quarks are massive, the chiral rotation generates another term in the action that can not be canceled by further field re-definitions, $m\bar{\psi}\psi \rightarrow m\bar{\psi}\psi + i\theta m\bar{\psi}\gamma_5\psi$, which is also P- and T-odd. Thus the CP-violating term in the QCD Lagrangian can be transformed between the gauge and fermion sectors, but it can not be eliminated.

Even though it cannot be eliminated, the θ term can be written as a total derivative [14],

$$\int d^4x \frac{g^2}{32\pi^2} \text{tr} [\varepsilon_{\mu\nu\rho\sigma} G^{\mu\nu} G^{\rho\sigma}] = Q, \quad (2.4)$$

where Q is the integral topological charge ($Q = 0, \pm 1, \pm 2, \dots$). Thus the θ term produces physical effects, like an electric dipole moment for the neutron.

Theoretical calculations naturally yield d_N in units of the unknown fundamental parameter θ . Thus to translate the current experimental bound to a constraint on θ , or to determine θ should a non-zero value of d_N be found through experiment, requires evaluation of nucleon matrix elements. The lattice regularization of QCD provides a first-principles technique for such calculations which we describe after discussing the chiral limit of d_N .

2.1 Taking the chiral limit

Consider the QCD partition function for N_f flavors of massive, degenerate, quarks after integrating over the Grassman quark fields,

$$Z = \int \mathcal{D}\mathcal{A}_\mu \det[\not{D}(m, \mathcal{A}_\mu) + i\theta m \gamma_5]^{N_f} e^{-S(\mathcal{A}_\mu)}, \quad (2.5)$$

where \mathcal{A}_μ is the gluon field, $\not{D}(m, \mathcal{A}_\mu)$ is a general covariant Dirac operator for a single quark flavor with mass m as may be found in the continuum or on the lattice. The choice of degenerate quarks is for convenience of notation with no loss of generality in the following. Factoring out $\det \not{D}(m, \mathcal{A}_\mu)$, the CP-even part of fermion action, and assuming θ is small,

$$\det[\not{D}(m, \mathcal{A}_\mu) + i\theta m \gamma_5] = \det[\not{D}(m, \mathcal{A}_\mu)] [1 + i\theta m \text{tr}(\gamma_5 \not{D}(m)^{-1})] + \mathcal{O}(\theta^2). \quad (2.6)$$

Next, using the spectral decomposition of the inverse Dirac operator and the Atiyah-Singer index theorem, we find $\text{tr}[\gamma_5 \not{D}^{-1}(m_f)] = Q/m$, so in the limit $m \rightarrow 0$, the θ term does not appear to vanish from the action, contradicting our above argument derived in the case where $m = 0$ from the start.

The seeming contradiction is easily resolved by examining the role of the usual (CP-even) fermionic action, $\det \not{D}(m, \mathcal{A}_\mu)^{N_f} = \prod_j (i\lambda_j + m)^{N_f}$. As $m \rightarrow 0$, $Q \neq 0$ configurations are suppressed since they support exact zero-modes of \not{D} with zero eigenvalue. In other words, in the chiral limit the $Q \neq 0$ configurations represent a set of measure zero, and the distribution of topological charge goes over to a delta-function, $\delta(Q)$, with zero width, $\langle Q^2 \rangle = 0$, so the θ term effectively vanishes.

The quenched approximation of Equation 2.6, $\det \not{D}(m, \mathcal{A}_\mu) = 1$, still allows CP-violating physics since the pseudoscalar density term in the action (or equivalently, the CP odd field-strength term) is not discarded (the same conclusion was reached in [18] through a different line of reasoning). However, in light of the arguments just made, the mass dependence of any observable depending on θ will be completely wrong, and one should expect significant systematic errors as a result. Indeed, the topological charge susceptibility, $\langle Q^2 \rangle/V$, which is closely related to d_N as we have just seen, is well known to be non-vanishing in the pure gauge theory [19].

2.2 Computational Methodology

The calculation of the dipole moments centers on the form factors that parameterize the matrix element of the electromagnetic current between nucleon states in the θ vacuum, $\langle p', s' | J^\mu | p, s \rangle_\theta = \bar{u}_{s'}(p') \Gamma^\mu(q^2) u_s(\vec{p})$ where

$$\Gamma^\mu(q^2) = \gamma^\mu F_1(q^2) + i\sigma^{\mu\nu} q_\nu \frac{F_2(q^2)}{2m} + (\gamma^\mu \gamma^5 q^2 - 2m\gamma^5 q^\mu) F_A(q^2) + \sigma^{\mu\nu} q_\nu \gamma^5 \frac{F_3(q^2)}{2m}. \quad (2.7)$$

$J^\mu = \frac{2}{3}\bar{u}\gamma^\mu u - \frac{1}{3}\bar{d}\gamma^\mu d$ is the electromagnetic current, $q = p' - p$ the space-like momentum ($q^2 < 0$) transferred by the external photon, s (s') the spin of the incoming (outgoing) nucleon, m the nucleon mass, $\sigma^{\mu\nu} \equiv i/2[\gamma^\mu, \gamma^\nu]$, and $u_s(\vec{p})$, $\bar{u}_{s'}(\vec{p})$ Dirac spinors.

The four terms on the right-hand side of Equation 2.7 are the most general set consistent with the Lorentz, gauge, and CPT symmetries of QCD. The insertion of J^μ probes the electromagnetic structure of the nucleon; for $q^2 \rightarrow 0$ it is easy to show that $F_1(0)$ is the electric charge of the nucleon in units of e (+1 for the proton, 0 for the neutron), $F_2(0)$ is the anomalous part of the magnetic moment, F_A is the anapole moment, and $F_3(0)$ gives the electric dipole moment. The last two vanish when $\theta \rightarrow 0$.

Later it will be useful to separate J^μ into its iso-scalar and iso-vector components.

$$J^\mu = \frac{1}{2}J_V^\mu + \frac{1}{6}J_S^\mu, \quad J_V^\mu = \bar{u}\gamma^\mu u - \bar{d}\gamma^\mu d, \quad J_S^\mu = \bar{u}\gamma^\mu u + \bar{d}\gamma^\mu d. \quad (2.8)$$

2.3 Calculating dipole moments on the lattice

For the case at hand, we study a three-point correlation function where a nucleon with spatial momentum \vec{p} is created at time 0 by the interpolating field $\chi_N^\dagger(0, \vec{p})$, the current is inserted at time t , and then the nucleon state is annihilated at time t' , $G^\mu(t', t) = \langle \chi_N(t', \vec{p}') | J^\mu(t, q) \chi_N^\dagger(0, \vec{p}) \rangle$. Inserting a complete set of relativistically normalized states between each interpolating field and the current and translating all fields to equal times, we obtain

$$G^\mu(t', t) = \sum_{s, s'} \langle 0 | \chi_N | p', s' \rangle \langle p', s' | J^\mu | p, s \rangle \langle p, s | \chi_N^\dagger | 0 \rangle \frac{1}{2E2E'} e^{-E'(t'-t)} e^{-Et} + \dots \quad (2.9)$$

$$= G^\mu(q) \times f(t, t', E, E') + \dots, \quad (2.10)$$

where "... " denote excited state contributions which we ignore. Note, the correlation function contains the desired S-matrix element, with no need to analytically continue back to Minkowski space-time. For convenience, we separate the correlation function into two parts, $G^\mu(q)$ which is a Dirac matrix, and $f(t, t', E, E')$ which collects all the kinematical factors, normalization of states, and time dependence of the correlation function. Color indices have been suppressed. The interpolating field χ_N is the conventional one used in most lattice simulations, *e.g.*, for the proton $\chi_P = \varepsilon_{abc} [u_a^T C \gamma_5 d_b] u_c$, with a, b , and c color indices.

The states are normalized conventionally, $\langle 0 | \chi_N^\dagger | p, s \rangle = \sqrt{Z_N} u_s(\vec{p})$, so using the spinor relation, $\sum_s u_s(\vec{p}) \bar{u}_s(\vec{p}) = E(\vec{p}) \gamma^t - i \vec{\gamma} \cdot \vec{p} + m$, and the projector $\mathcal{P}^{xy} = \frac{i}{4} \frac{1+\gamma^t}{2} \gamma^x \gamma^y$, setting $\vec{p}' = 0$ and $\theta = 0$, we find the magnetic form factor $G_M(q^2) = F_1(q^2) + F_2(q^2)$, up to known kinematical factors.

$$\text{tr } \mathcal{P}^{xy} G^x(q^2) = p_y m (F_1(q^2) + F_2(q^2)), \quad \text{tr } \mathcal{P}^{xy} G^y(q^2) = -p_x m (F_1(q^2) + F_2(q^2)). \quad (2.11)$$

Similarly, the electric form factor $G_E(q^2) = F_1(q^2) + \frac{q^2}{(2m)^2} F_2(q^2)$ is found from

$$\text{tr } \mathcal{P}^t G^t(q^2) = m(E + m) \left(F_1(q^2) + \frac{q^2}{(2m)^2} F_2(q^2) \right), \quad \mathcal{P}^t = \frac{1}{4} \frac{1 + \gamma^t}{2}. \quad (2.12)$$

Throughout this talk we include the factor $(1 + \gamma^t)/2$ in projectors to yield the positive parity state (neutron or proton in the CP-even vacuum) (see, *e.g.* [20]).

To determine the desired moment, or form factor, the factor $f(t, t', E, E')$ appearing in Equation 2.10 must be removed from the correlation function. This is most easily done by taking a ratio

with another suitably chosen three-point function. For example, taking the ratio of Equation 2.11 with Equation 2.12 yields the magnetic dipole moment of the nucleon in the limit $q^2 \rightarrow 0$.

$$\lim_{t' \gg t \gg 0} \frac{1}{p_y} \frac{\text{tr} \mathcal{P}^{xy} G_{P,N}^x(t, t', E, \vec{p})}{\text{tr} \mathcal{P}^t G_P^t(t, t', E, \vec{p})} = \frac{1}{p_y} \frac{\text{tr} \mathcal{P}^{xy} G_{P,N}^x(q^2)}{\text{tr} \mathcal{P}^t G_P^t(q^2)} + \dots \quad (2.13)$$

$$= \frac{1}{E+m} \frac{F_1(q^2) + F_2(q^2)}{G_E^{(P)}(q^2)} + \dots \quad (2.14)$$

$$\lim_{q \rightarrow 0} \frac{1}{E+m} \frac{F_1(q^2) + F_2(q^2)}{G_E^{(P)}(q^2)} = \frac{1}{2m} \times \begin{cases} 1 + a_{\mu,P} \\ a_{\mu,N} \end{cases}. \quad (2.15)$$

where we have used $F_1(0) = 1$ for the proton and 0 for the neutron, and $a_\mu = F_2(0)$ is the anomalous part of the moment. P and N denote proton and neutron, respectively, and the denominator is always evaluated for the proton. Because we take ratios corresponding to different components of the electromagnetic current, the finite renormalization constant associated with the local lattice current² drops out and need not be calculated.

2.4 CP violating vacuum, $\theta \neq 0$

In this section we consider the case $\theta \neq 0$. First, we must explain a somewhat subtle issue concerning mixing of the magnetic and electric dipole moment terms in correlation functions arising from the physical mixing of the CP-even vacuum eigenstates $|N\rangle$ ($P = +1$) and $|N^*\rangle$ ($P = -1$)[9, 21]³ when $\theta \neq 0$.

$$|N^\theta\rangle = |N\rangle + i\alpha'|N^*\rangle. \quad (2.16)$$

Here, $|N^\theta\rangle$ is the neutron state in the CP broken vacuum, and α' is a small mixing angle that is proportional to θ . This physical mixing of states gives rise to an *unphysical* mixing of the electric and magnetic dipole moment form factors in correlation functions like those given in Equation 2.9. Generally, the mixing in Equation 2.16 can be written as a Dirac spinor with phase $e^{i\alpha\gamma_5}$ ($\alpha \propto \alpha'$) since $\gamma_5 u_s(\vec{p}) = v_s(\vec{p})$, *i.e.*, γ_5 takes a spinor of a given parity into the other⁴. One obtains

$$\sum_{s,s'} u_{s',\theta}(\vec{p}) \bar{u}_{s,\theta}(\vec{p}) = E(\vec{p}) \gamma_t - i\vec{\gamma} \cdot \vec{p} + m e^{2i\alpha\gamma_5} \approx E(\vec{p}) \gamma_t - i\vec{\gamma} \cdot \vec{p} + m(1 + 2i\alpha\gamma_5), \quad (2.17)$$

where $u_{s,\theta}(\vec{p}) \equiv e^{i\alpha\gamma_5} u_s(\vec{p})$. We have assumed that $\alpha \ll 1$. Using $u_{s,\theta}(\vec{p})$ in (2.9) instead of $u_s(\vec{p})$ and proceeding as in the previous section, we obtain

$$\text{tr} \mathcal{P}^{xy} G^z(q^2) = \alpha m(E-m)F_1 + \alpha(m(E-m) + \frac{p_z^2}{2})F_2 + \frac{p_z^2}{2}F_3 + \mathcal{O}(\theta^2) \quad (2.18)$$

$$\text{tr} \mathcal{P}^{xy} G^t(q^2) = ip_z \left(\alpha m F_1(q^2) + \alpha \frac{E+3m}{2} F_2(q^2) + \frac{E+m}{2} F_3(q^2) \right) + \mathcal{O}(\theta^2). \quad (2.19)$$

²On the lattice only the point-split form of the current is conserved. Here we use a local definition, $\bar{\psi} \gamma_\mu \psi$.

³In a preliminary report on this work[13], we did not account for this mixing. We are grateful to M. Pospelov and S. Aoki for pointing this out to us. The mixing occurs because we work with correlation functions, not directly with matrix elements constructed from CP eigenstates.

⁴Parity is defined for particles in the rest frame.

These equations can be used to extract the electric dipole form factor $F_3(q^2)$. In particular, taking the ratio of Equation 2.19 with the proton electric form factor correlation function, Equation 2.12, we arrive at

$$\frac{1}{ip_z} \frac{\text{tr} \mathcal{P}^{xy} G_N^t(t, t', E, \vec{p})}{\text{tr} \mathcal{P}^t G_P^t(t, t', E, \vec{p})} = \frac{1}{ip_z} \frac{\text{tr} \mathcal{P}^{xy} G_{P,N}^t(q^2)}{\text{tr} \mathcal{P}^t G_P^t(q^2)} + \dots \quad (2.20)$$

$$= \frac{\alpha m F_1(q^2) + \alpha \frac{E+3m}{2} F_2(q^2) + \frac{E+m}{2} F_3(q^2)}{m(E+m) G_E^{(P)}(q^2)} + \dots \quad (2.21)$$

Subtracting the F_1 and F_2 terms and taking the limit $q^2 \rightarrow 0$ yields the electric dipole moment.

$$\frac{F_3(q^2)}{2m G_E^{(P)}(q^2)} = \left\{ \frac{1}{ip_z} \frac{\text{tr} \mathcal{P}^{xy} G_N^t(t, t', E, \vec{p})}{\text{tr} \mathcal{P}^t G_P^t(t, t', E, \vec{p})} - \frac{\alpha m F_1(q^2) + \alpha \frac{E+3m}{2} F_2(q^2)}{m(E+m) G_E^{(P)}(q^2)} \right\} \quad (2.22)$$

$$d_N = \frac{F_3(0)}{2m} = \lim_{q^2 \rightarrow 0} \left\{ \frac{1}{ip_z} \frac{\text{tr} \mathcal{P}^{xy} G_N^t(t, t', E, \vec{p})}{\text{tr} \mathcal{P}^t G_P^t(t, t', E, \vec{p})} - \frac{\alpha m F_1(q^2) + \alpha \frac{E+3m}{2} F_2(q^2)}{m(E+m) G_E^{(P)}(q^2)} \right\}. \quad (2.23)$$

The value of the mixing angle α is most easily calculated from the ratio of the zero momentum two-point functions[21].

$$\langle \chi_{N^\theta}(t) \chi_{N^\theta}^\dagger(0) \rangle_\theta = \frac{\langle 0 | \chi_{N^\theta} | N^\theta \rangle \langle N^\theta | \chi_{N^\theta}^\dagger | 0 \rangle}{2m_{N^\theta}} e^{-m_{N^\theta} t} + \dots = Z_{N^\theta} \sum_{s, s'} \frac{u_{s, \theta}(0) \bar{u}_{s', \theta}(0)}{2m_{N^\theta}} e^{-m_{N^\theta} t} + \dots, \quad (2.24)$$

where, as usual, "... " denotes excited state contributions. Using the spinor relation (2.17) and appropriate projectors,

$$\text{tr} \frac{1 + \gamma_t}{2 \cdot 4} \langle \chi_{N^\theta}(t) \chi_{N^\theta}^\dagger(0) \rangle_\theta \approx Z_N e^{-m_N t}, \quad (2.25)$$

$$\text{tr} \frac{1 + \gamma_t}{2 \cdot 4} \gamma_5 \langle \chi_{N^\theta}(t) \chi_{N^\theta}^\dagger(0) \rangle_\theta \approx i Z_N \alpha e^{-m_N t}, \quad (2.26)$$

to lowest order in θ . Note that $Z_{N^\theta} = Z_N + \mathcal{O}(\theta^2)$ and $m_{N^\theta} = m_N + \mathcal{O}(\theta^2)$, and as θ is very small in Nature, we work only to lowest order. Of course, the right-hand side of the first equation is nothing but the usual ground state contribution to the nucleon two-point function computed in the CP even vacuum.

A final comment is in order. As explained clearly in [9], one is free to include in the action the $i\theta' m \bar{\psi} \gamma_5 \psi$ mass term, arising from a chiral rotation on the quark fields through a particular choice of basis, in addition to the $-i\theta Q$ term used here. Physical observables will depend only on the combination $\bar{\theta} \equiv \theta + \theta'$, and the mixing effects, like those described above, will differ in just the right way to ensure this is so. In other words, the chiral rotation affects the quark fields in Equation 2.16 as well as in the action. It is only the relative strength, or difference (note the opposite signs of the two terms), of the two contributions that leads to physical effects.

2.5 Computing with $\theta \neq 0$

The $\theta \neq 0$ action, being complex, is difficult to simulate with conventional lattice methods. However, this problem can be avoided by working in the small θ limit,

$$\langle \mathcal{O} \rangle_\theta = \frac{1}{Z(\theta)} \int \mathcal{D}\mathcal{A}_\mu \mathcal{D}\bar{\psi} \mathcal{D}\psi \mathcal{O} e^{-S(\mathcal{A}_\mu) - i\theta \int d^4x \frac{g^2}{32\pi^2} \text{tr}[G(x)\tilde{G}(x)]} \quad (2.27)$$

$$\approx \frac{1}{Z(0)} \int \mathcal{D}\mathcal{A}_\mu \mathcal{D}\bar{\psi} \mathcal{D}\psi (1 - i\theta Q) \mathcal{O} e^{-S(\mathcal{A}_\mu)} = \langle \mathcal{O} \rangle - i\theta \langle Q\mathcal{O} \rangle \quad (2.28)$$

where \mathcal{O} is a generic operator functional of the fields. Note $\langle \mathcal{O} \rangle_\theta$ becomes an expectation value in the CP-even vacuum, the CP-odd part weighted over topological sectors⁵

$$\langle Q\mathcal{O} \rangle = \sum_{\mathbf{v}} P(Q_{\mathbf{v}}) Q_{\mathbf{v}} \langle \mathcal{O} \rangle_{\mathbf{v}}, \quad (2.29)$$

where $P(Q)$ is the probability that the gauge field configuration has charge Q . As before, the electric dipole moment, or any CP-odd observable, is seen to be closely related to the topological charge, and we expect that any such observable should vanish as $\langle Q^2 \rangle / V \rightarrow 0$. In [23] this was shown explicitly for the large N limit. Chiral perturbation theory shows that $d_N \sim m_\pi^2 \log m_\pi^2$ [6] and $\langle Q^2 \rangle / V \sim m_\pi^2$ [24], so each vanishes in the chiral limit, as expected.

Finally, the mixing angle α must also vanish as $m_\pi^2 \rightarrow 0$ since it is proportional to θ ; this will happen as $\langle Q^2 \rangle / V \rightarrow 0$. It bears repeating that in the quenched case $\langle Q^2 \rangle / V$ is independent of the quark mass, implying that d_N and α do not vanish in the chiral limit.

3. Results

We begin by investigating the topological charge on the ensemble of $N_f = 2$ gauge configurations. Figure 1 shows the simulation time history of Q ; evidently there are long autocorrelations, a fact already noted in [12]. The lower panel corresponds to a quenched simulation ($a^{-1} \approx 1.3$ GeV) where Q fluctuates rapidly. Note the abscissa is different in the quenched case. The difference in fluctuations reflects the fact that the quenched lattices are separated by 1000 sweeps, whereas the dynamical ones are separated by only five trajectories, owing to the significantly higher cost of the latter. In the former case, one sweep = one heat-bath plus four over-relaxed hits on each link of the lattice. In the latter, one trajectory = 50 steps of hybrid molecular dynamics evolution of each link plus one global Metropolis accept/reject step. We also emphasize that the suppression of tunneling between topological sectors is an algorithmic, not physics, problem which is much worse in the dynamical case due to the smooth hamiltonian evolution of the Monte-Carlo algorithm (see also [25, 26] for earlier studies of this problem using staggered fermions). The method used to calculate Q uses APE smearing with coefficient 0.45 for twenty steps and an improved definition of the lattice field strength (see [12] for details). An even better approach may be to use the overlap definition of the topological charge [27], though the precise definition of Q is probably not the limiting factor.

In Figure 1b, the topological susceptibility χ is shown for both quenched and $N_f = 2$ cases, the former being plotted as a horizontal line since it does not depend on any sea quark mass (the $N_f = 2$ results were determined from the data in [12], the quenched from [28]). χ and m_π are plotted in units of the Sommer scale, r_0 , to the appropriate power to make each dimensionless. The values for r_0 were taken from [12] ($N_f = 2$) and [28] (quenched). The interesting feature to note is the significant decrease of the $N_f = 2$ value relative to the quenched one. While there may be some

⁵In [22] it has been proposed to use the pseudo-scalar density as a weight instead. For chirally symmetric lattice fermions that have an index, this is equivalent to weighting with Q . If chiral symmetry is broken, then the two methods will agree in the limit $a \rightarrow 0$.

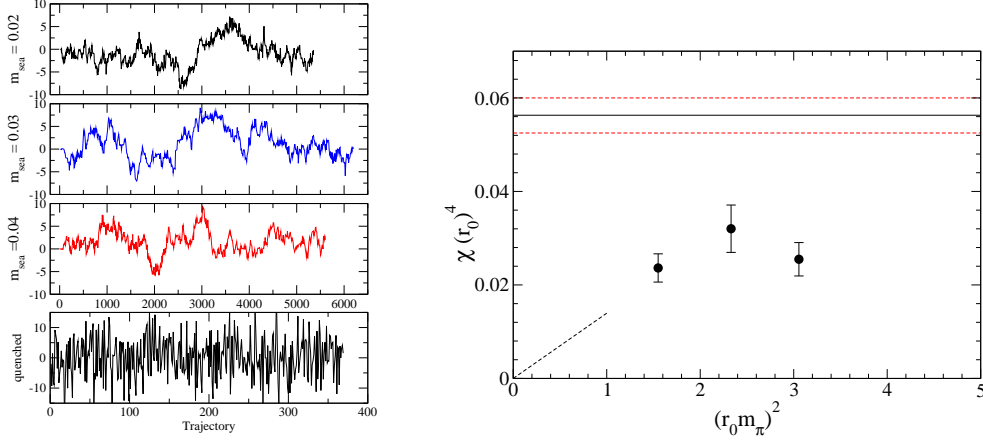


Figure 1: (a) Topological charge, Q . For the $N_f = 2$ simulations, Q for every fifth trajectory is shown, while for the quenched case Q has been measured on lattices separated by 1000 sweeps. The $N_f = 2$ plots are reproduced from [12]. (b) Topological charge susceptibility for $N_f = 2$ (filled circles) and quenched (solid line and horizontal dashed lines). The dashed line is the chiral perturbation theory prediction, with $r_0 f$ evaluated from [12]. Results are given in terms of the Sommer scale, r_0 , for convenience.

sea quark mass dependence, χ levels off between $m_{sea} = 0.03$ and 0.04 . In addition, the statistical errors shown in the figure were estimated by blocking the data in groups of 50 trajectories (10 lattices) and treating the blocks as independent while Figure 1 indicates the topological charge has autocorrelations on longer scales. Also shown in Figure 1b is the prediction from lowest order chiral perturbation theory. It is comforting that this lowest order prediction is consistent with the $N_f = 2$ lattice calculation, but because of the caveats just made, the agreement is not yet significant. Given the close relation between χ and the quark mass dependence of the electric dipole moment, it does not seem promising that the mass dependence of d_N can be accurately determined from these ensembles; (much) longer evolutions are required. Nevertheless, the $m_f = 0.04$ calculation may give a relatively good estimate of the magnitude of d_N in QCD where the lightest quark mass is about m_s . From Figure 1b, this is almost surely *not* true for the quenched case.

Next we discuss the CP even and odd parts of the two-point function (Equations 2.25 and 2.26). Again, working to lowest order in θ by weighting expectation values with iQ in the latter case, the masses and Z factors obtained from each *must* be equal. To reduce statistical errors, we average the forward and backward in time parts of the nucleon propagator⁶. For the usual $\theta = 0$ propagator, this means averaging positive and negative parity states (particle and anti-particle). For $\theta \neq 0$, the particle and anti-particle states have the same CP-odd part containing both parities (*c.f.*, Equation 2.17). Thus, we fit to

$$G_{\text{even}}(t, \vec{p}) = A e^{-E(\vec{p})t}, \quad G_{\text{odd}}(t, \vec{p}) = A \left(e^{-E(\vec{p})t} - e^{-E(\vec{p})(N_t-t)} \right), \quad (3.1)$$

for the former and latter, respectively, in the range $7 \leq t \leq 12$ to avoid excited state contamination. Ignoring the excited state contributions is justified by the acceptable χ^2/dof of the single particle

⁶We omitted the negative parity states from our earlier discussion and Equation 2.24 for clarity. The backward propagating, negative parity, anti-particle state appears because of the anti-periodic boundary condition in time (see [20]).

fits. For the CP odd case, the χ^2/dof is a bit large, but likely for different reasons that are explained below. This averaging is equivalent to performing a time-reversal transformation on the correlation function which, in turn, is equivalent to averaging over time-reversed gluon configurations. This last step flips the sign of the topological charge on the underlying gluon configuration (recall that the θ term is odd under time-reversal). Thus, performing the average of forward and backward correlation functions has the same effect as exactly symmetrizing the topological charge distribution of the ensemble.

Though not shown, the measured values of $E(p)$ from the CP even part of the two point function compare well to the continuum relativistic dispersion relation, $E(p) = \sqrt{\vec{p}^2 + m_N^2}$, with either $p_i = 2\pi n/L_i$ or $\sin(p_i)$ ($n = 0, \pm 1, \pm 2, \dots, \pm L_i - 1$), the latter being the exact lattice momentum for a free fermion with a naive nearest neighbor action. The agreement is satisfactory for small $|\vec{p}|$, indicating lattice artifacts are small in this case. Thus, in the following we simply use $p_i = 2\pi n/L_i$ for the momentum. Since this would lead to large $\mathcal{O}(a^2)$ errors for large $|\vec{p}|$, we restrict our analysis to the four non-zero lowest values admitted on our lattice, $\vec{n} = (1, 0, 0)$, $(1, 1, 0)$, $(1, 1, 1)$, and $(2, 0, 0)$ and permutations. Since the larger momentum correlation functions are considerably more noisy anyway and suffer large $\mathcal{O}(a^2)$ errors with either choice, this is not a cause for concern.

In Figure 2a we show the nucleon mass versus the minimum time slice used in the fit. Values of m_N for both CP even and odd parts of the two-point function are shown. For $t_{min} > 4$, they are roughly constant within statistical errors. In the range $5 \leq t_{min} \leq 12$ the masses clearly disagree outside statistical errors; the difference in central values is roughly ten percent. The value of χ^2/dof for the CP-odd case is roughly two, while in the CP-even case it is less than one. A naive ratio of the two-point functions, which would give the mixing angle α if the masses were equal, is also shown in Figure 2a (lower panel). Although a plateau appears at small t_{min} , the ratio appears to decrease approximately linearly with t in the region where the masses are constant but unequal, as expected. Given our discussion of the topological charge, these results are not surprising. Since our topological charge distribution is symmetric by the argument given above, it must be the shape of the distribution for $|Q|$ that is not correct, presumably due to insufficient sampling.

To check this possibility, we calculated the same two-point functions on a quenched ensemble of lattices. As mentioned already, the topological charge distribution on this ensemble is expected to be correct in quenched QCD because many more Monte-Carlo updates have been performed between measurements. The masses obtained from fits like those in the dynamical case are shown in Figure 2b. The masses agree within statistical errors for $t > 5$ and the difference of the central values is less than five percent, so now the naive ratio provides a relatively accurate value of the mixing angle, $\alpha = 0.214(32)$, where the error is statistical only, and we have averaged over the range $5 \leq t \leq 10$. All of the fits for both CP-even and odd parts of the correlation function have $\chi^2/\text{dof} < 1$. This test of agreement of the masses is a simple, but non-trivial, check that the distribution of Q is correct. While the quenched result is clearly an improvement over the two flavor one, Figure 2 suggests that an even more accurate sampling of Q is desirable.

One way to proceed in the $N_f = 2$ case is to fit each correlator separately, extract the coefficient of the ground state exponential from the large time region and then take the ratio of these coefficients to determine α . One can take the mass in the CP odd case as a free parameter or fix it to the correct value from the CP even case. Though this is more correct than just taking the ratio

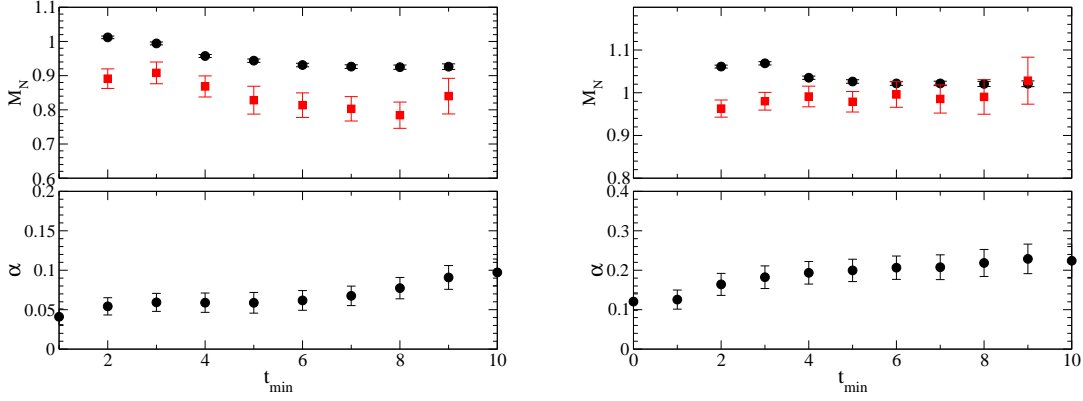


Figure 2: (a) Upper panel: nucleon mass from single particle fits to the CP-even (circles) and odd (squares) parts of the two-point correlation function; t_{min} is the value of the smallest time slice used in the fit. Lower panel: mixing angle α from the simple ratio of the same CP-odd and even parts of the two-point correlation function. $m_{sea} = 0.04$. (b) Same as (a) but for the quenched simulation.

of correlation functions and picking out the incorrect plateau, it will still yield a value of α with some significant systematic error. After all, the fitted masses differ by about ten percent. Likewise, we may anticipate the value of α to be incorrect by this amount. Being a bit more systematic, let us say the correlation function itself has been determined close its actual value. Then we make a ten percent error in the amplitude (and therefore α) since the fitted mass is ten percent too low. Now, a reasonable guess may be that the correlation function is actually determined to roughly ten percent of its correct value. Taking both factors into account, we arrive at a systematic uncertainty in α of about 10-20%. Following this procedure gives $\alpha \sim 0.072(15)$ (statistical error only). Here, m_N in the CP odd part of the correlation function has been fixed to the CP even value, and α is from the fit with $t_{min} = 7$. If m_N is left as a free parameter, the resulting value of α is about 50% lower. The systematic uncertainties just described notwithstanding, we conclude that the $N_f = 2$ value of α is significantly smaller than the quenched value. Again, this conclusion is buttressed by the significant difference in the topological susceptibilities in the two cases.

We now turn to the ratios of the three-point correlation functions given in Equations 2.13 and 2.20. In Figure 3 we show the magnetic and subtracted electric dipole moment ratios for the neutron for each value of q^2 . For magnetic form factors we average results using both equations in 2.11. Despite the flat plateaus shown in the figures, some excited state contamination may still be present at small and large times, given the fitted masses in Figure 2a. For the largest momentum transfer, the plateaus show an oscillation, presumably due to insufficient statistics, or possibly excited state contamination. The ratios $F_{1,2}(q^2)/G_E^{(P)}(q^2)$ and $F_3(q^2)/(2mG_E^{(P)}(q^2))$ are summarized in Table 1. The value of the F_1 ratio for the neutron approaches zero, as required by electric charge conservation. For the proton, the ratio trivially approaches one since it goes to $F_1(0)/F_1(0)$, but, at the least, it serves as a check on our evaluation of the three-point functions.

As $q^2 \rightarrow 0$, the $F_2(q^2)$ ratios yield the anomalous magnetic moments of the nucleons. For each value of q^2 the magnitudes for the neutron and proton are equal within errors; this should be true for the iso-vector contributions, assuming iso-spin is not broken which is true in our calcu-

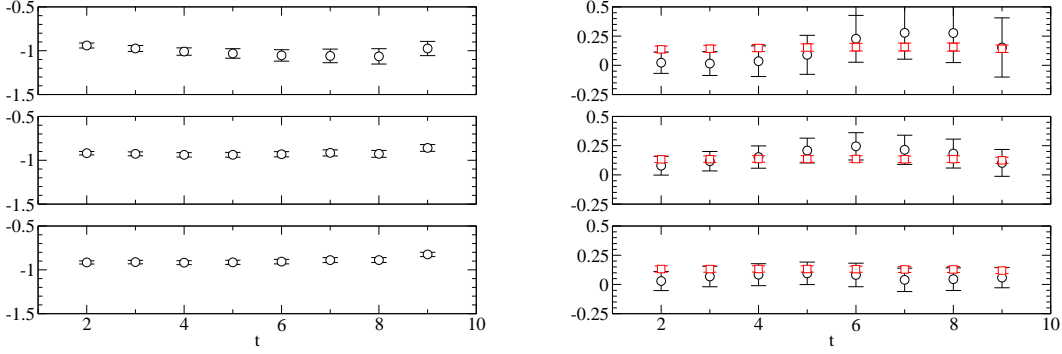


Figure 3: (a) Ratio of three-point functions given in Equation 2.13 that yields the magnetic dipole moment of the neutron in the limit $q^2 \rightarrow 0$. Plots are shown for units of lattice momenta, $\vec{q} = (1, 0, 0)$, $(1, 1, 0)$, and $(1, 1, 1)$, and permutations, in the lower, middle, and upper panels respectively. $m_{sea} = 0.04$. (b) The ratio $(F_3(q^2)/2m)/G_E(q^2)$ (Equation 2.22). In the limit $q^2 \rightarrow 0$ this ratio yields the electric dipole moment of the neutron. Also shown is the subtraction term (squares) in Equation 2.22.

Table 1: Form factors normalized by the electric form factor of the proton, $G_E(q^2)$ (Equation ??). In the limit $q^2 \rightarrow 0$, the values in the F_2 columns yield the anomalous magnetic moments and in the last column, the electric dipole moment of the neutron.

q^2 (GeV ²)	$F_1(q^2)/G_E(q^2)$		$F_2(q^2)/G_E(q^2)$		$(F_3(q^2)/2m)/G_E(q^2)$
	proton	neutron	proton	neutron	neutron
0.401	1.0695 (42)	-0.045 (7)	1.703 (59)	-1.715 (46)	0.087 (95)
0.753	1.1349 (89)	-0.081 (13)	1.760 (66)	-1.785 (52)	0.202(103)
1.044	1.2181 (223)	-0.102 (27)	2.050 (129)	-2.013 (101)	0.117 (160)
1.538	1.2107 (414)	-0.156 (45)	1.345 (195)	-1.409 (136)	-0.287 (249)

lation. Evidently the iso-scalar contribution from the connected diagrams is zero, or smaller than our statistical errors; we have not included the disconnected valence quark loop diagrams in the three-point functions which contribute only to the matrix element of the iso-scalar piece of the electromagnetic current. The values at the lowest value of q^2 are not far off from the well known experimentally measured values $a_\mu^{(P)} = 1.79$ and $a_\mu^{(N)} = -1.91$ [29]. To show the momentum dependence of these ratios is mild and to compare to experiment [30], we have also plotted the ratio of the magnetic form factors to the electric form factor of the proton, $G_M(q^2)/G_E^{(P)}(q^2)$, as well as the dipole moments in Figure 4a. The agreement with the experimental form factor ratio for the proton is quite satisfactory, in magnitude and q^2 dependence but may be fortuitous since our calculation does not include electromagnetic effects or disconnected valence quark loop contributions, is at a single relatively heavy quark mass, and we have not taken the continuum or infinite volume limits.

Finally, the $q^2 \rightarrow 0$ limit of the $F_3(q^2)$ ratio yields $|d_N|$. Our value is consistent with zero, within errors, except at the middle value of q^2 where the central value is roughly two standard deviations from zero. There is no significant dependence on q^2 outside of our large statistical uncertainties (Figure 4b). The lack of precision in d_N/θ stems mainly from two related sources,

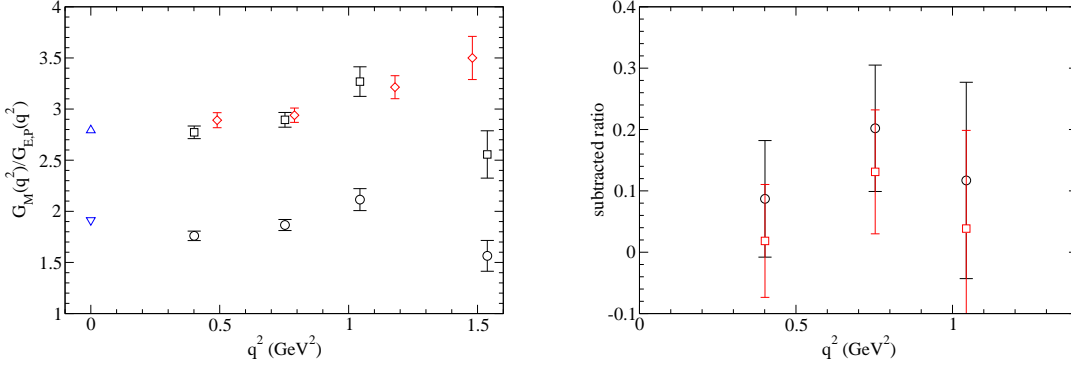


Figure 4: (a) Ratios of the proton (squares) and neutron (circles) magnetic form factors to the proton electric form factor (Equation 2.14 times $E + m$). The limit $q^2 \rightarrow 0$ yields the magnetic moments. The absolute value is plotted for the neutron for comparison. $m_{sea} = 0.04$. The diamonds are experimental data points [30] where we have added quoted statistical and systematic errors in quadrature. The triangles at $q^2 = 0$ are the experimentally measured magnetic moments [29] (the absolute value for the neutron (lower triangle) is shown). (b) The ratio in Equation 2.20 after subtraction of the unphysical mixing with the magnetic dipole moment term. The electric dipole moment of the neutron, $F_3(0)/2m$, is obtained as $q^2 \rightarrow 0$.

insufficient statistics and a systematic error in the extraction of the mixing (angle) between CP-even and odd states in the $\theta \neq 0$ vacuum. The second error can also rightly be thought of as resulting from poor statistics, or sampling, of the topological charge in the $N_f = 2$ simulations. The remedy for both is simple, just run longer simulations.

Extrapolation of the above subtracted ratio to $q^2 = 0$ seems a pointless exercise given the large statistical and systematic uncertainties. Thus we simply estimate the $q^2 = 0$ value as the one at the lowest value of momentum transfer,

$$d_N^{\text{lat}} = \frac{F_3(0)}{2m} \approx \frac{F_3(0.401 \text{ GeV}^2)}{2m} = +0.087(95).$$

The quoted error is statistical only. The mild q^2 dependence for the F_1 and F_2 ratios lead us to believe that this is not a terrible approximation. Our conventions which are the same as those in [6, 7] have lead to a positive central value of d_N/θ . This could well change as the precision of future calculations improves.

d_N^{lat} is given in inverse units of $a\theta$. In physical units, $d_N \approx 0.010(11) \theta e \text{ fm}$. This central value is roughly an order of magnitude larger than the one computed from sum rules [9], a factor of two times as large as the (leading) pion-loop contribution [6], and about a factor of two smaller than the quenched value reported in [11].

Using the current experimental bound on d_N [1], our central value of d_N implies

$$\theta = \frac{d_N^{\text{expt}}}{d_N^{\text{lat}}} \lesssim 6.3 \times 10^{-11} \quad (3.2)$$

for the fundamental CP-odd parameter in the QCD action.

Future lattice calculations will approach the chiral limit, which will suppress d_N^{lat} further. Chiral perturbation theory predicts a leading $m_\pi^2 \log m_\pi^2$ term [6], but non-leading m_π^2 terms may also be important [7, 8, 9], so we cannot reliably extrapolate our result to the physical point with only one mass. Lighter quark mass simulations similar to the present one are now in progress to address this question. We note that a recent calculation [31] may help with these extrapolations.

Because d_N arises from the CP-odd term in the action, $\int d^4x G\tilde{G}$, it is sensitive to the topological charge distribution. As discussed in Section 2.1, in the quenched case it will not have the correct quark mass dependence. In the two flavor case, the quark mass dependence is correct, and d_N vanishes in the chiral limit from the presence of the CP even part of the fermion determinant.

$N_f = 2 + 1$ flavor domain wall fermion calculations just begun jointly by the RBC and UKQCD collaborations will attempt to address the two most pressing deficiencies of the present calculation, poor statistics for the topological charge and the quark mass dependence of d_N . We are also extending the current $N_f = 2$ study to quark masses as light as $m_{\text{strange}}/2$.

Acknowledgments

We thank Norman Christ and Sinya Aoki for helpful discussions. Calculations were carried out on the RIKEN BNL Research Center QCDSF supercomputer.

References

- [1] P. G. Harris *et al.*, *New experimental limit on the electric dipole moment of the neutron*, *Phys. Rev. Lett.* **82** (1999) 904–907.
- [2] J. Bijnens and E. Pallante, *Weak long distance contributions to the neutron and proton electric dipole moments*, *Phys. Lett.* **B387** (1996) 207–214, [[hep-ph/9606285](#)].
- [3] **BNL** Collaboration, Y. Semertzidis, *Proposed searches for electric dipole moments of the muon, deuteron and proton in storage rings*, *Talk given at the APS 2005 April Meeting* (2005).
- [4] **ANL** Collaboration, I. Ahmad, *Electric dipole moment of ^{225}Ra* , <http://www-mep.phy.anl.gov/atta/research/radiumedm.html> (2005).
- [5] V. Baluni, *Cp violating effects in qcd*, *Phys. Rev.* **D19** (1979) 2227–2230.
- [6] R. J. Crewther, P. Di Vecchia, G. Veneziano, and E. Witten, *Chiral estimate of the electric dipole moment of the neutron in quantum chromodynamics*, *Phys. Lett.* **B88** (1979) 123.
- [7] S. Aoki and T. Hatsuda, *Strong cp violation and the neutron electric dipole moment revisited*, *Phys. Rev.* **D45** (1992) 2427–2436.
- [8] A. Pich and E. de Rafael, *Strong cp violation in an effective chiral lagrangian approach*, *Nucl. Phys.* **B367** (1991) 313–333.
- [9] M. Pospelov and A. Ritz, *Theta induced electric dipole moment of the neutron via QCD sum rules*, *Phys. Rev. Lett.* **83** (1999) 2526–2529, [[hep-ph/9904483](#)].
- [10] P. Faccioli, D. Guadagnoli, and S. Simula, *The neutron electric dipole moment in the instanton vacuum: Quenched versus unquenched simulations*, *Phys. Rev.* **D70** (2004) 074017, [[hep-ph/0406336](#)].

- [11] E. Shintani *et al.*, *Neutron electric dipole moment from lattice qcd*, *Phys. Rev.* **D72** (2005) 014504, [[hep-lat/0505022](#)].
- [12] Y. Aoki *et al.*, *Lattice qcd with two dynamical flavors of domain wall fermions*, [hep-lat/0411006](#).
- [13] F. Berruto, T. Blum, K. Orginos, and A. Soni, *Neutron electric dipole moment with domain wall quarks*, *Nucl. Phys. Proc. Suppl.* **140** (2005) 411–413, [[hep-lat/0411003](#)].
- [14] S. R. Coleman, *The uses of instantons*, . Lecture delivered at 1977 Int. School of Subnuclear Physics, Erice, Italy, Jul 23-Aug 10, 1977.
- [15] K. Fujikawa, *Path integral measure for gauge invariant fermion theories*, *Phys. Rev. Lett.* **42** (1979) 1195.
- [16] M. Creutz, *Spontaneous cp violation and quark mass ambiguities*, [hep-lat/0410043](#).
- [17] M. Creutz, *Ambiguities in the up-quark mass*, *Phys. Rev. Lett.* **92** (2004) 162003.
- [18] S. Aoki, A. Gocksch, A. V. Manohar, and S. R. Sharpe, *Calculating the neutron electric dipole moment on the lattice*, *Phys. Rev. Lett.* **65** (1990) 1092–1095.
- [19] E. Witten, *Current algebra theorems for the $u(1)$ 'goldstone boson'*, *Nucl. Phys.* **B156** (1979) 269.
- [20] S. Sasaki, T. Blum, and S. Ohta, *A lattice study of the nucleon excited states with domain wall fermions*, *Phys. Rev.* **D65** (2002) 074503, [[hep-lat/0102010](#)].
- [21] S. Aoki, Y. Kuramashi, and E. Shintani *Talk given at the ILFTNetwork Workshop on Lattice QCD and Phenomenology, Tsukuba* (2004).
- [22] D. Guadagnoli, V. Lubicz, G. Martinelli, and S. Simula, *Neutron electric dipole moment on the lattice: A theoretical reappraisal*, *JHEP* **04** (2003) 019, [[hep-lat/0210044](#)].
- [23] D. Diakonov, M. V. Polyakov, and C. Weiss, *Hadronic matrix elements of gluon operators in the instanton vacuum*, *Nucl. Phys.* **B461** (1996) 539–580, [[hep-ph/9510232](#)].
- [24] B. Billeter, C. DeTar, and J. Osborn, *Topological susceptibility in staggered fermion chiral perturbation theory*, *Phys. Rev.* **D70** (2004) 077502, [[hep-lat/0406032](#)].
- [25] B. Alles, G. Boyd, M. D'Elia, A. Di Giacomo, and E. Vicari, *Hybrid monte carlo and topological modes of full qcd*, *Phys. Lett.* **B389** (1996) 107–111, [[hep-lat/9607049](#)].
- [26] B. Alles *et al.*, *Scanning the topological sectors of the qcd vacuum with hybrid monte carlo*, *Phys. Rev.* **D58** (1998) 071503, [[hep-lat/9803008](#)].
- [27] L. Giusti, G. C. Rossi, M. Testa, and G. Veneziano, *The $u(1)_a$ problem on the lattice with ginsparg-wilson fermions*, *Nucl. Phys.* **B628** (2002) 234–252, [[hep-lat/0108009](#)].
- [28] Y. Aoki *et al.*, *Domain wall fermions with improved gauge actions*, *Phys. Rev.* **D69** (2004) 074504, [[hep-lat/0211023](#)].
- [29] **Particle Data Group** Collaboration, S. Eidelman *et al.*, *Review of particle physics*, *Phys. Lett.* **B592** (2004) 1.
- [30] **Jefferson Lab Hall A** Collaboration, M. K. Jones *et al.*, *$G(e(p))/g(m(p))$ ratio by polarization transfer in $e(\text{pol.}) p \rightarrow e p(\text{pol.})$* , *Phys. Rev. Lett.* **84** (2000) 1398–1402, [[nucl-ex/9910005](#)].
- [31] D. O'Connell and M. J. Savage, *Extrapolation formulas for neutron edm calculations in lattice qcd*, [hep-lat/0508009](#).